coatings

MDPI

Article

Enhanced Corrosion Protection of Epoxy/ZnO-NiO Nanocomposite Coatings on Steel

Muna Ibrahim, Karthik Kannan, Hemalatha Parangusan, Shady Eldeib, Omar Shehata, Mohammad Ismail, Ranin Zarandah and Kishor Kumar Sadasivuni *

Centre for Advanced Materials, Qatar University, Doha P.O. Box 2713, Qatar; mi1701758@qu.edu.qa (M.I.); karthik.kannan@qu.edu.qa (K.K.); hemakavin@gmail.com (H.P.); se1608668@qu.edu.qa (S.E.); os1602469@qu.edu.qa (O.S.); mi1507960@qu.edu.qa (M.I.); rz1403631@qu.edu.qa (R.Z.)
* Correspondence: kishorkumars@qu.edu.qa; Tel.: +974-5058-0237

Received: 14 June 2020; Accepted: 8 August 2020; Published: 12 August 2020

Abstract: ZnO-NiO nanocomposite with epoxy coating on mild steel has been fabricated by the sol–gel assisted method. The synthesized sample was used to study corrosion protection. The analysis was performed by electrochemical impedance spectroscopy in 3.5% NaCl solution. The structural and morphological characterization of the metal oxide nanocomposite was carried out using XRD and SEM with Energy Dispersive Absorption X-ray (EDAX) analysis. XRD reveals the ZnO-NiO (hexagonal and cubic) structure with an average ZnO-NiO crystallite size of 26 nm. SEM/EDAX analysis of the ZnO-NiO nanocomposite confirms that the chemical composition of the samples consists of: Zn (8.96 ± 0.11 wt.%), Ni (10.53 ± 0.19 wt.%) and O (80.51 ± 3.12 wt.%). Electrochemical Impedance Spectroscopy (EIS) authenticated that the corrosion resistance has improved for the nanocomposites of ZnO-NiO coated along with epoxy on steel in comparison to that of the pure epoxy-coated steel.

Keywords: ZnO-NiO; nanocomposite; steel coatings; epoxy resin; anticorrosion; corrosion inhibition mechanism

1. Introduction

At the moment stainless steel can play an imperative role in a human lifetime by being used in applications like cars and chemical factories. Mild steel has been chosen because it has good mechanical properties but at the same time, can prevent the corrosion process. Corrosion can be the main reason for industrial accidents. Corrosion attacks the material by interaction with the environment [1]. Corrosive elements such as water, ions, and oxygen are competent at exceeding all coatings of a polymer. Epoxy resin is employed to protect the steel in most of the common polymers owing to its adhesion, chemical resistivity, mechanical and dielectric properties. Because of wear and abrasion of surface, metals with epoxy coatings are easily degraded. Pure epoxy coated metals exhibit extremely feeble corrosion resistance due to the convoluted cross-linked structure. Hence, various nanostructured fillers were employed to boost the defending properties of epoxy coatings.

Nanostructured materials are recognized for their exceptional physical and mechanical properties owing to their tremendously fine grain size and huge grain boundary volume. In past few years, bi and tri-metal oxide nanocomposites have been an area of vigorous integrative research, owing to their extensive technological purposes. Metal oxide nanocomposites provide the rewards of unique physical and chemical properties. The adherence of a composite coating was established to be imperative in the anticipation of corrosion and transfer in open circuit potential to the anodic site. The outstanding enhancement in the recital of these coatings has been linked with the enhancement of the barrier to dissemination, preclusion of charge transport by metal oxide nanomaterials [2].

The metal oxide coating is broadly utilized for anticorrosion owing to its inexpensive manufacture, effortlessness of function, and superior anticorrosive property [3]. Metal oxide coatings offer conciliatory protection to steel reports with outstanding wear, abrasion, and corrosion resistance. Fabrication of bi and tri-metal oxide composite coatings is an excellent option for improving the service life of steel [4]. Many examinations have reported composite coating enclosing various metal oxide nanoparticles such as ZnO, SnO_2, TiO_2, ZrO_2, Al_2O_3, NiO, CeO_2, SiO_2, CrO_3, etc., which demonstrated advanced properties of excellent thermal stability, shelf life, wear resistance, hardness and corrosion resistance [5,6]. There are ample published papers with research work related to that of metal oxide nanoparticles for corrosion resistance. For instance, Boomadevi Janaki et al. have used nano-alumina encapsulated epoxy coated on mild steel, which was confirmed by Electrochemical Impedance Spectroscopy (EIS) and scanning electrochemical microscopy (SECM) with a 3.5% NaCl solution [7]. They improved nanoparticles of the alumina by modification of their surface and analyzed it by Fourier transform infrared spectroscopy, concluding that the resistance of corrosion for alumina epoxy nanocomposites coated on the mild steel can be improved. Therefore, chemical reactions that can be evolved amid epoxy and surface of alumina nanoparticles in composites give high fortification properties and ionic resistances [8–11]. By using analyses like SEM with EDAX, they have shown the presence of metals like Fe, Al, and O in the corrosion products. Hardness and tensile strength tests also proved that they have improved mechanical properties for alumina epoxy nanocomposite coated on mild steel.

Nowadays, mixed metal oxide composites have shown noteworthy chemical and physical properties compared to distinct metal oxide nanoparticles for multifunctional applications. Popolla et al. have accounted the corrosion studies (superior hardness, corrosion and wear resistance) of a Zn-ZnO-Y_2O_3 composite coating [12]. The Zn-ZnO-Cr_2O_3 coating showed higher hardness and anticorrosion behavior when investigated by Fayomi et al. [13]. Malatji et al. have accounted for the superior corrosion resistance behavior of a mixed metal oxide Zn-Al_2O_3-CrO_3-SiO_2 nanocomposite exhibiting excellent corrosion resistance behavior [14]. Preparation of CeO_2 doped ZnO nanoparticle composite coatings on mild steel have been reported by Kallappa et al. [15].

NiO is a superior reinforcing metal oxide and displays excellent corrosion resistance properties. Nanostructured NiO has a lesser thermal conductivity and its composite with metal oxide coatings displayed excellent corrosion resistance. Wadhwani et al. have demonstrated the enhanced corrosion inhibitive effect of NiO nanoparticles for mild steel in an acid medium [16]. Synthesis, characterization, and anticorrosion studies of spray-coated NiO thin films have been reported by Shajudheen et al. [17]. The behavior of Ni/CeO_2 nanocomposite coatings via the electrodeposition route for anticorrosion has been accounted by Aruna et al. [18]. Leaf extract mediated NiO nanoparticles for anticorrosive applications were reported by Suresh et al. [19]. Yu-Jun et al. have stated that Ni–CeO_2 composite coatings have excellent tribological performance [20]. Comparison of anticorrosive studies of spray-coated TiO_2 and NiO thin films has been performed by Shajudheen et al. [21]. Deng et al. have reported the corrosion behavior of electrodeposited Ni and Cu nanocrystalline foils with the influence of UV light irradiation [22]. ZnO-NiO nanocomposites having plentiful exceptional parameters, such as corrosion resistance, large surface area, thermal conductivity, broad potential windows etc., are a glowing ensemble for corrosion studies. Various techniques have been accessed for the fabrication of ZnO-NiO nanocomposites such as thermal composition, hydrothermal, co-precipitation, sol–gel, spray pyrolysis methods, etc. [12–22]. Among these methods, the sol–gel assisted route is simple and also does not involve many control parameters, multistep processes, etc. Hence, the anticorrosive studies of the present mixed metal oxide composite are fabricated by the sol–gel assisted route. Only a few pieces of the mixed metal oxide composite research works have focused on corrosion protection in recent years.

Based on the recent reports, the anticorrosion behavior of nanostructured ZnO-NiO with epoxy composite has not been exhaustively studied so far. So, this paper aims to fabricate ZnO-NiO with Epoxy nanocomposites by the sol–gel assisted route and an examination of the structural (XRD),

morphology (SEM with EDAX), and electrochemical (corrosion protection) properties of the prepared ZnO-NiO-epoxy nanocomposite coatings on mild steel has been carried out.

2. Experimental

2.1. Materials

All the chemicals: zinc acetate hexahydrate (99% purity), nickel nitrate hexahydrate (99% purity), sodium hydroxide (>98% purity) (for the synthesis of ZnO-NiO nanocomposite), sodium chloride (99% purity), and chloroform (99% purity) used for the preparation of electrolytes were of analytical grade and obtained from Sigma Aldrich. Bisphenol-A epoxy resin (LAPOX*C-51), and hardener (LAPOX AH-428) were obtained from Atul Limited, India for coating purposes.

2.2. Preparation of ZnO/NiO Nanocomposite

The ZnO and NiO nanoparticles were prepared by the sol–gel assisted method. A representative sol–gel assisted synthesis process was approved for the fabrication of a ZnO/NiO nanocomposite. An amount of 0.5 M of zinc acetate and 1 M of sodium hydroxide were dissolved in double distilled water (DD) to form solution A. A total of 0.5 M of nickel nitrate and 1 M of sodium hydroxide were dissolved in DD to form solution B. Then, solution B was included dropwise into the solution A. In order to achieve a homogenous solution, the prepared mixed solution was vigorously stirred for 5 h and made into a blackish gel. The resulting blackish gel was mixed with DD and centrifuged at 7000 rpm for 30 min followed by washing with DD and ethanol three times to remove the impurities. The black-colored product was kept on a hot plate for ignition and heated at 150 °C (six h). To acquire nanocrystalline powder, this was sintered at 400 °C for 4 h. A fine black colored powder was attained, and this was carefully collected for additional characterization purposes.

2.3. Preparation of Pure Epoxy

Epoxy resin (EM 9500) and curing agent (EM 9520) were mixed in the ratio of 3:1; this mixture was degassed in a bath sonicator. It was then coated into a steel substrate and permitted to dry for 24 h at room temperature.

2.4. Preparation of Epoxy/ZnO/NiO Nanocomposites

Amounts of 1 and 1.8%-ZnO/NiO nanopowder was dispersed in 5 mL chloroform using an ultrasonicator for 30 min. Then the solution was mixed with Epoxy resin and stirred overnight. The homogenous mixture was placed over the hot plate at 80 °C until the chloroform evaporated. After this, the mixture was degassed for 10 min and hardener was included in the mixture and mixed well. The adopted epoxy: the Hardener-mixing ratio was 3:1. Then the final mixture was coated on a steel substrate and dried at room temperature. The above synthesis steps were used to prepare Epoxy/ZnO-NiO composite samples with different concentrations of ZnO/NiO (1 and 2.5%).

2.5. Different Steps for the Preparation of Epoxy with Metal Oxide Composites

An amount of 0.06 g of ZnO-NiO powder was added to 5 mL of chloroform. The mixed solution was sonicated for 30 min. An amount of 3 mL of Resin was added to the sonicated solution under constant stirring for 24 h. After 24 h, 1 mL of Hardener was added in the above solution and stirred again for 1 h.

2.6. Corrosion Behavior of Steel Before and After the Coating

Corrosion is the interface between the metal and the environment, which will damage the properties of the metal itself. Interaction between the metal and oxygen can cause the formation of oxide layers. Electrochemical instruments can tell us if the materials that we coat in the metal can prevent corrosion or not. We tested the steel with a nanocomposite epoxy polymer in an electrochemical

instrument with NaCl solution to test for electrical conductivity. The principle behind this being, the lower the current the current the better the protection from corrosion. We checked coated steel, and it showed that the epoxy prevented corrosion well. In addition, the nanocomposite played a good role in the prevention of corrosion.

2.7. Characterization

The fabricated ZnO-NiO nanocomposite was inspected via morphological and structural analysis. The crystallinity, crystal structure, physical parameters (lattice constant, crystallite size, and dislocation density) of the synthesized ZnO-NiO nanocomposite were analyzed by using X-ray diffraction analysis. The XRD pattern was examined by the X'PERT-Pro MPD, PANalytical Co., Almelo, Netherlands diffractometer equipped with CuKα radiation (1.5404 Å), using a step scanning mode and a tube voltage of 40 kV and a current of 15 mA. The scanning range varies between 10° and 80°, with the scanning rate (2°/min) and sampling rate (0.04°/min), varying correspondingly. Morphological studies were conducted by scanning electron microscopy (SEM). In the SEM analysis, the accelerating voltage was 5 kV and the working distance was attuned to approximately 6 mm. The contrast and brightness of the images were set to the most favorable values so that particles could be effortlessly distinguished from the background. Energy Dispersive Absorption X-ray (EDAX) analysis is a technique of elemental analysis connected to electron microscopy supported by the creation of characteristic X-rays that discloses the occurrence of elements present in the specimens. The SEM used has an in built EDAX (SEM, Hitachi S-4800, Hitachi, Tokyo, Japan).

2.8. Electrochemical Experiments

Initially the samples were coated on well-polished steel sheets using single-layer smart coatings (SLSCs). The electrochemical measurements were executed in a double-jacketed cell with the three-electrode system. Epoxy with ZnO-NiO nanocomposite was utilized as a working electrode. Ag/AgCl and graphite rods were employed as counter and reference electrode, respectively. All electrochemical experiments were carried out in 3.5 wt.% NaCl saturated solution with diverse concentrations of the prepared composites using (reference 3000, Gamry Co., Warminster, PA, USA). Steel was dunked into the 3.5% NaCl solution for 30 min to accomplish the balanced state for the metal with the solution before each testing. The EIS analyses were performed in a frequency of 0.1 Hz to 100 kHz with AC amplitude of 10 mV using a reference 3000, Gamry Co., USA. The potentiodynamic polarization plots were accomplished versus the reference electrode potential.

3. Results and Discussion

3.1. Structural and Morphological Analysis of the ZnO/NiO Composite

The XRD diffractogram of the ZnO, NiO, and ZnO-NiO nanocomposite is depicted in Figure 1. The XRD results show that the ZnO-NiO nanocomposite contains hexagonal ZnO and cubic NiO phases. The diffractions peaks located at 31.77°, 34. 45°, 36.15°, 47.58°, 56.60°, 66.45°, 68.03°, and 69.13° are in good accordance with the ZnO standard crystal planes (1 0 0), (0 0 2), (1 0 1), (1 0 2), (1 1 0), (2 0 0), (1 1 2) and (2 0 1). The other peaks located at 37.06°, 42.96°, 62.92°, 74.85°, and 78.87° correspond to NiO crystal planes (1 0 1), (0 1 2), (1 1 0), (1 1 3) and (2 0 2). The pattern obtained conforms well to the standard JCPDS (Joint Committee on Powder Diffraction Standards) card number 89-1397 (ZnO) and 89-7130 (NiO). The physical parameters attained for the synthesized ZnO-NiO nanocomposite are presented in Table 1. There were no contamination peaks detected in the XRD pattern, which proves the superior clarity in the synthesized ZnO-NiO nanocomposite. The average crystallite size (D) of the composite was computed through the Debye Scherrer formulae followed by estimation of the dislocation density (δ) [22].

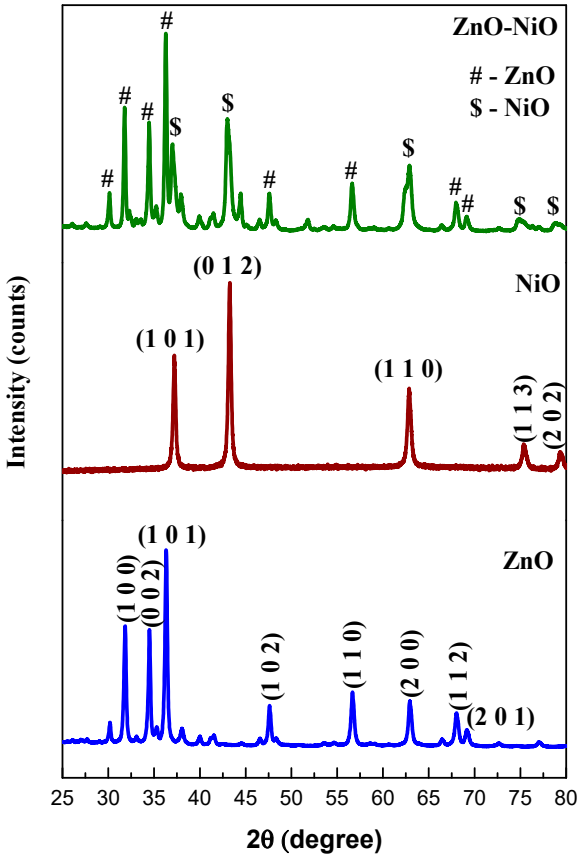

Figure 1. XRD pattern of ZnO, NiO nanoparticles and ZnO-NiO nanocomposite.

Table 1. Physical parameters calculated from XRD data of nanocomposite.

Material	Phases	Lattice Constant (nm)	D (nm) $D = k\lambda/\beta\cos\theta$	$(\delta) \times 10^{14}$ (Lines/m^2) $\delta = 1/D^2$
ZnO	hexagonal	a = 0.3234 c = 0.5165	41	5.95
NiO	cubic	a = 0.4175	28	12.8
ZnO-NiO	ZnO (hexagonal)	a = 0.4218 c = 0.5191	34	8.65
	NiO (cubic)	a = 0.4170	18	30.9

The SEM micrographs of the ZnO-NiO nanocomposite with different magnifications are shown in Figure 2a,b. The surface of the nanocomposite was not smooth. At 10KX magnification, the average grain size of the powder was revealed to be around 100 nm. Figure 2a illustrates the SEM image at a higher enlargement and it can be observed that the particles were detained collectively owing to feeble physical forces. Here, particles were produced with sizes in the micron range. Figure 2b shows the SEM images at a higher enlargement, and it can be observed that particles of sizes less than 100 nm were produced. It also provides an understandable idea about the particle separation, which can be seen from the fact that the particles are divided effortlessly and not extremely influenced by agglomeration. The composite with Ni was not demonstrated to have a remarkable outcome on the particle size of ZnO. Since Ni ions were isolated onto the surface of ZnO, they might have control over the growth to minute grains [23]. As seen in Figure 2a,b, particles with different sizes were present in the nanocomposite powder.

The EDAX spectrum of the ZnO-NiO nanocomposite (Figure 2c) confirms that the chemical composition of the samples consists of Zn (8.96 ± 0.11 wt.%), Ni (10.53 ± 0.19 wt.%) and O (80.51 ± 3.12 wt.%). It was found that the chemical composition corresponded to the requirement and EDAX validates the effective incorporation of Ni into the ZnO nanoparticles [23]. No contamination peaks were present in the spectra representing the chemical purity of the sample.

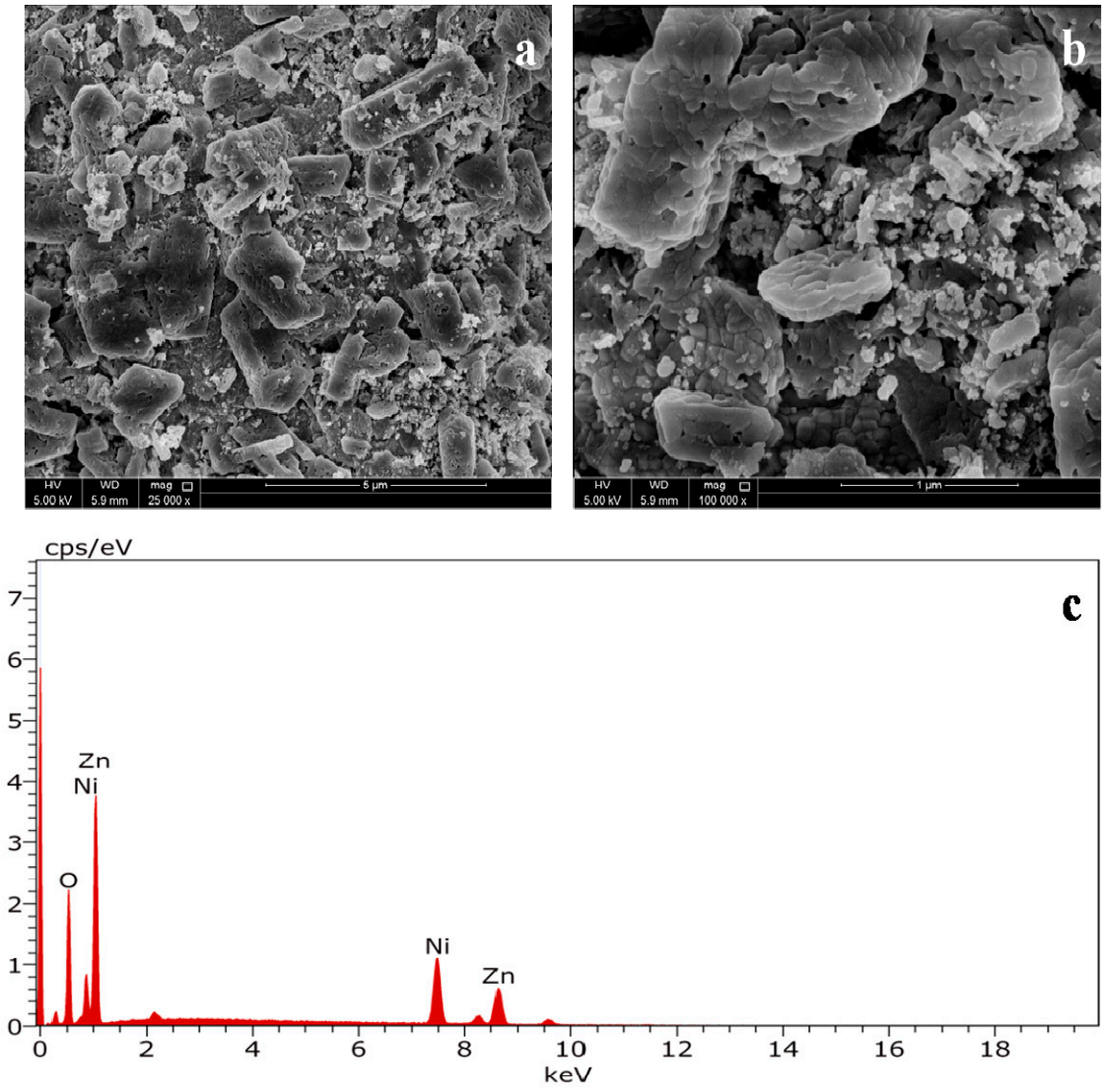

Figure 2. (**a**,**b**) SEM with different magnifications and (**c**) Energy Dispersive Absorption X-ray (EDAX) images of ZnO-NiO nanocomposite.

3.2. Potentiodynamic Polarization (PP) Characterization

The corrosion fortification performances of the steel, epoxy, EP/1 ZnO-NiO, and EP/1.8 ZnO-NiO nanocomposite coatings were estimated by EIS and Potentiodynamic polarization measurements. The Tafel plots of the steel, epoxy, EP/1 ZnO-NiO, and EP/1.8 ZnO-NiO nanocomposite coatings subjected to 3.5% NaCl solution are illustrated in Figure 3. It can be seen from the figures that there was change in Tafel slope plots, and this was owing to the passive layer arrangement on steel. It can be seen that the EP/1.8 ZnO-NiO nanocomposite coating demonstrated superior resistance to that of other coated samples. The epoxy customized ZnO-NiO coated steel was not active in the direction of the corrosion reaction as can be observed from Figure 3. The corrosion parameters computed from Tafel plots are illustrated in Table 2. The Tafel plots demonstrate that the EP/1.8 ZnO-NiO had the lowest

corrosion current and rate. As a result, it had the uppermost corrosion protection in contrast to the other tested coatings. Furthermore, the corrosion potential of the EP/1.8 ZnO-NiO altered in a positive direction, which represents greater protection behavior. This is owing to the constraints placed on the progress of corrosive ions to the substrate by the deposition of boosted cross-linked chemical structures and improved dispersion on surface modified using the ZnO-NiO composite [24–28]. This acted as a strong physical barrier. This behavior develops the corrosion resistance rate (CR). As a result, the CR of epoxy tailored ZnO-NiO nanocomposite coatings was established to be very low compared to that of the samples without surface modification coating. The outcome verifies that pure epoxy and epoxy-based nanocomposites (different ratio) diminished the CR [29–32].

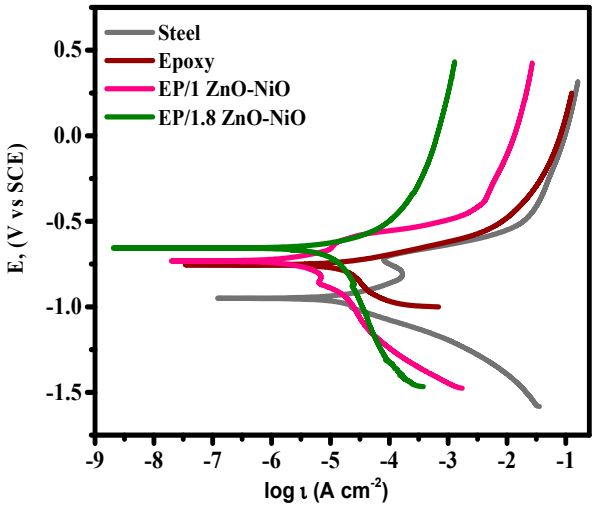

Figure 3. Potentiodynamic polarisation illustration for the steel, epoxy, epoxy/1.0 ZnO-NiO, and epoxy/1.8 ZnO-NiO nanocomposites.

Table 2. Electrochemical data for different specimens from Tafel fitting.

Samples	E_{corr} (V)	I_{corr} (μA/cm^2)	b_a (V/Decade)	b_c (V/Decade)	Corrosion Rate (mpy)
Steel	−0.97	95.49	0.38	0.42	43.99
Epoxy	−0.91	18.62	0.21	0.36	8.57
EP/1 ZnO-NiO	−0.79	13.18	0.12	0.17	6.07
EP/1.8 ZnO-NiO	−0.68	5.37	0.11	0.11	2.47

3.3. EIS Characterization

The corrosion resistance of the nanocomposites coatings was premeditated by EIS analysis. Figure 4 reveals the Nyquist plots of steel, epoxy, EP/1 ZnO-NiO, and EP/1.8 ZnO-NiO nanocomposite coatings in 3.5% NaCl solution. The curve appears as a two-time constant semicircle because of the permeation of a corrosive medium through the defects or pores, coming out in under-film corrosion and coating delamination. The low-frequency impedance displays the elevated stability of the coatings through immersion.

The corrosion performance of the bare steel was considered the baseline position. The EP/ZnO-NiO composite illustrated excellent corrosion inhibition compared to that of steel as the Epoxy layer nearly enclosed the steel surface and formed a physical barrier that obstructs the transmission of the ions from the salt solution. In EP/1.8 ZnO-NiO, the impedance value at small frequency was improved when compared to that of Epoxy. This is accredited to the superior interfacial contact of ZnO-NiO with epoxy via the surface functionalities, good ZnO-NiO dispersion, and the long convoluted corridor for the stabbing molecules [33–37].

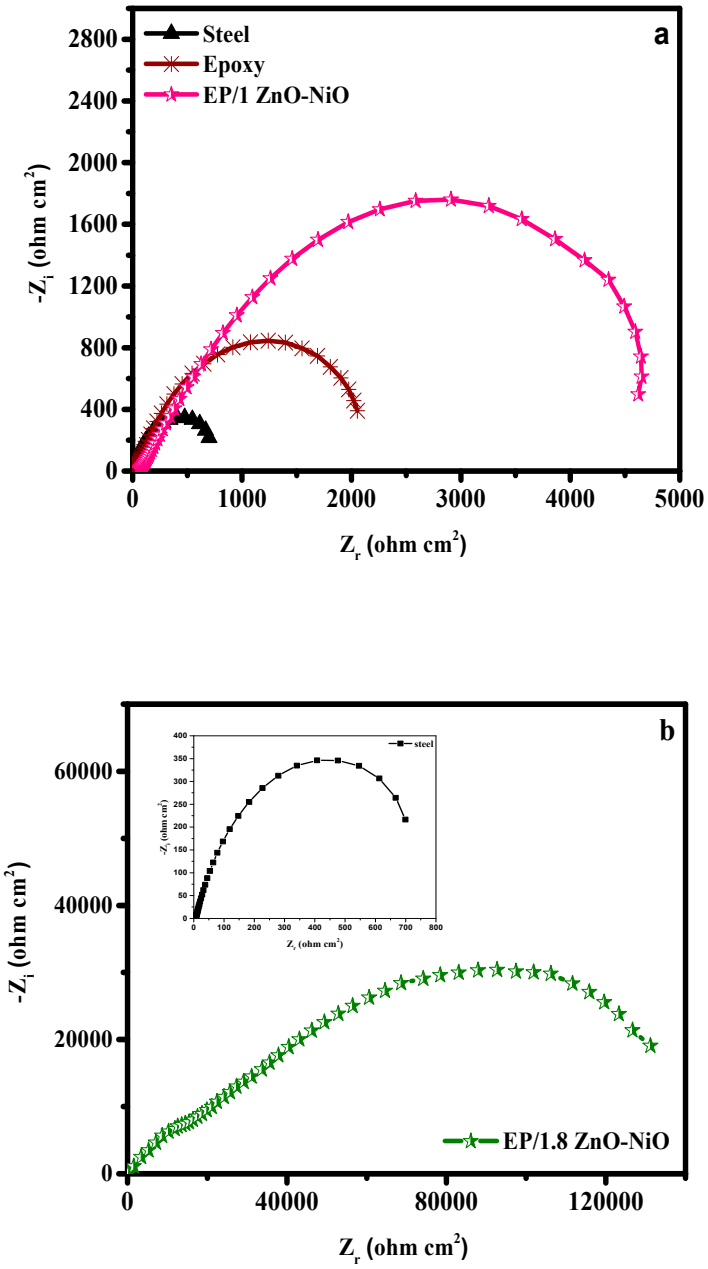

Figure 4. (**a**) Nyquist plots attained for steel, epoxy and EP/1.0 ZnO-NiO nanocomposites and (**b**) EP/1.8 ZnO-NiO nanocomposite coated mild steel submerged in 3.5% NaCl solution (inset: Nyquist plot of steel).

Figure 5 illustrates Bode and phase angle plots for steel, epoxy, EP/1 ZnO-NiO, and EP/1.8 ZnO-NiO nanocomposite coatings. It is evident that the EP/1.8 ZnO-NiO nanocomposite coating demonstrates the utmost maximum phase angle and impedance change from the low to the high-frequency region compared to the pure epoxy and EP/1 ZnO-NiO coated samples. The EP/1.8 ZnO-NiO nanocomposite coated mild steel had superior charge transfer resistance compared to pure epoxy and EP/1 ZnO-NiO coated samples. It can be observed that the EP/1.8 ZnO-NiO coating displayed an enlarged time constant in the series of the high frequencies that is accredited to its improved barrier properties [38–40]. As can be seen from Table 3, the EP/1.8 ZnO-NiO nanocomposite coatings exhibited superior anticorrosive performance when compared to other reported nanomaterials and thin film coating systems.

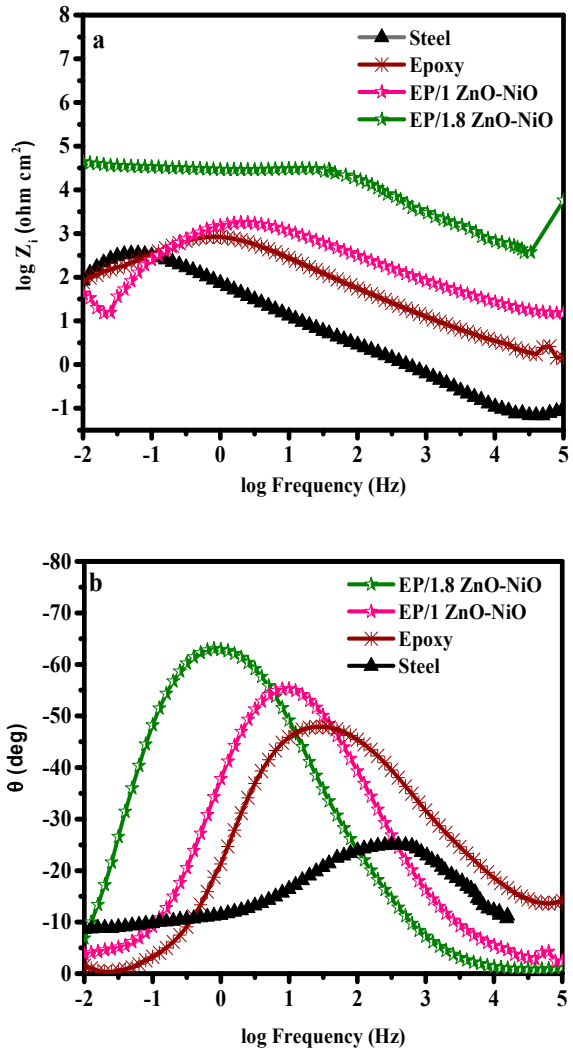

Figure 5. (**a**,**b**) Bode plots acquired for steel, epoxy and EP/1.0 ZnO-NiO nanocomposite coated mild steel immersed in 3.5% NaCl solution.

3.4. Corrosion Inhibition Mechanism

The projected illustration of the corrosion protection mechanism of the nanocomposites on the metal surface is shown in Figure 6. Since the corrosion procedure in an unbiased chloride solution can be performed with an anodic route of suspension of Fe and a decrease in the cathodic route of O_2 and H_2O, OH^- can be produced; Fe_2O_3 is then created via a series of the chemical oxidation route. Diverse materials for corrosion protection were produced and found from the restrained nature of the corrosion effect, such as evading O_2 and H_2O diffusion onto the metal composite surface and hindering metal oxidation. Significant study of the mechanism of corrosion protection with nanocomposite materials can be categorized as follows: (i) the high surface energy owing to nanomaterials system guides the creation of appropriate surface irregularity and hydrophobic surfaces at the top of the Epoxy/1.8 ZnO-NiO coating, and (ii) the formation of an adjacent interconnecting structure with tough adhesion at the coating–composite interface [54–58].

The former of these experiments reproduced the aqueous corrosive ions from the surface of the Epoxy/1.8 ZnO-NiO coating, while the latter generated an impediment in the dissemination of the ionic electrolyte, which created the notable corrosion defensive capability in the nanostructured metal oxide composite coatings [59–68].

Table 3. Comparison of the corrosion parameters of different nanomaterial coatings.

Sample	Substrate	Medium	E_{corr} (V)	I_{corr} ($\mu A/cm^2$)	Ref.
TiO_2 nanoparticles	316L stainless steel	0.5 mol/L NaCl solution	−0.117	0.783	[41]
Amorphous TiO_2 nanoparticles (CrN/TiO_2)	316L stainless steel	3 wt.% NaCl solution	−0.49	0.00031	[42]
Ta_2O_5 thin films	Carbon steel	0.2 M NaCl solution	−0.671	0.0348	[43]
Al_2O_3 thin films	Copper	0.5 M NaCl solution	−0.308	2.71	[44]
ZrO_2 thin films	316L stainless steel	1M H_2SO_4 solution	−0.1814	3.11	[45]
CS/GO-OA	Carbon steel	3.5 wt.% NaCl solution	−0.374	3.9	[46]
Graphene/polyaniline	Mild steel	0.1 M HCl (pH = 1)	−0.532	0.572	[47]
Al_2O_3/Ni	Mild steel	3.5 wt.% NaCl solution	−0.253	0.011	[48]
SiC/Ni	Carbon steel	0.5 M Na_2SO_4	−0.2605	1.9	[49]
TiO_2-Ni-Zn-P	Low carbon steel	3.5 wt.% NaCl solution	−0.404	0.364	[50]
SiC-Ni	Copper	3.5 wt.% NaCl solution	−0.248	0.6645	[51]
SiC-Ni-P	St37 tool steel	3.5 wt.% NaCl solution	−0.255	1.58	[52]
SiO_2-Ni-P	API-5LX65 steel	3.5 wt.% NaCl solution	−0.336	0.308	[53]
EP/1.8 ZnO-NiO	Steel	3.5 wt.% NaCl solution	−0.68	5.37	Present study

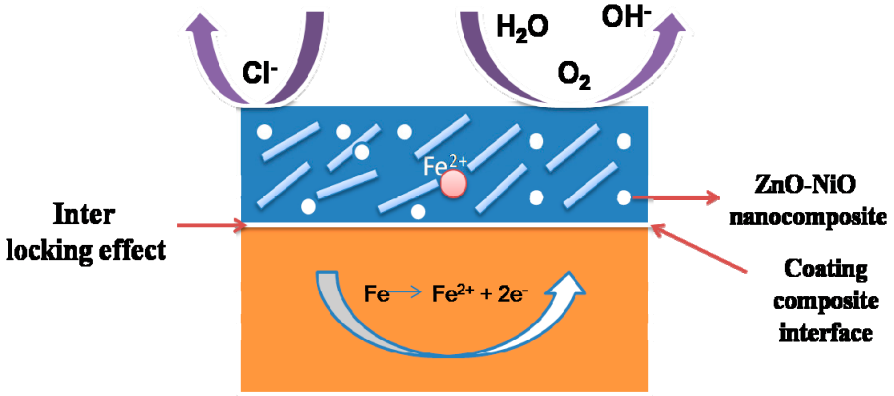

Figure 6. Proposed mechanism of the corrosion protection by the metal oxide (ZnO-NiO) nanocomposite.

4. Conclusions

In this work, the sol–gel assisted ZnO-NiO nanocomposite and its structural, morphological, and compositional properties were investigated. XRD revealed a hexagonal ZnO - cubic NiO arrangement with an average crystallite size of 26 nm. SEM images confirmed the agglomerated particles with sizes of less than 100 nm of the prepared composite. EIS and PP experiment results established that the ZnO-NiO with Epoxy coating has the superior anticorrosion capability. EIS studies demonstrated higher charge and resistance for the epoxy/1.8–ZnO-NiO nanocomposite coated steel. The improved anticorrosion performance was exhibited by the EP/1.8 ZnO-NiO–epoxy coating compared to the pure epoxy, EP/1 ZnO-NiO coatings. This could be accredited to the surface alteration of the ZnO-NiO composite to speed up the probable chemical communications between the composite and epoxy matrix. The anticorrosion (Epoxy/1.8 ZnO-NiO) coating has outstanding physical barrier qualities, which can be employed in the corrosion protection field.

Author Contributions: Conceptualization, K.K.S., H.P., M.I. (Muna Ibrahim), and K.K.; methodology, K.K.S., H.P., M.I. (Muna Ibrahim), K.K., S.E., O.S., M.I. (Mohammad Ismail), and R.Z.; validation, K.K.S., H.P., and M.I. (Muna Ibrahim); formal analysis, H.P., M.I. (Muna Ibrahim), S.E., O.S., M.I. (Mohammad Ismail), and R.Z.;

investigation, K.K.S., H.P., and K.K.; writing—original draft preparation, K.K., M.I. (Muna Ibrahim), and H.P.; writing—review and editing, K.K., H.P., and K.K.S.; supervision, K.K.S.; project administration, K.K.S. All authors have read and agreed to the published version of the manuscript.

Funding: This research was funded by the Undergraduate Research Experience Program project no. UREP24-133-2-036 from the Qatar National Research Fund (a member of Qatar Foundation). The statements made herein are solely the responsibility of the authors.

Acknowledgments: This work was supported by the UREP grant # UREP24-133-2-036 from the Qatar National Research Fund (a member of Qatar Foundation). The statements made herein are solely the responsibility of the authors. The authors would like to thank the Central laboratory Unit (CLU), Qatar University, 2713, Doha, Qatar, for SEM with EDAX analysis facility.

Conflicts of Interest: The authors declare no conflict of interest.

References

1. Javidparvar, A.A.; Naderi, R.; Ramezanzadeh, B. Manipulating graphene oxide nanocontainer with benzimidazole and cerium ions: Application in epoxy-based nanocomposite for active corrosion protection. *Corros. Sci.* **2020**, *165*, 108379. [CrossRef]
2. Aslam, J.; Mobin, M.; Aslam, R.; Ansar, F. Corrosion protection of low carbon steel by conducting terpolymer nanocomposite coating in 3.5 wt% NaCl solution. *J. Adhes. Sci. Technol.* **2020**, *34*, 443–460. [CrossRef]
3. Shen, L.; Li, Y.; Zhao, W.; Wang, K.; Ci, X.; Wu, Y.; Liu, G.; Liu, C.; Fang, Z. Tuning F-doped degree of rGO: Restraining corrosion-promotion activity of EP/rGO nanocomposite coating. *J. Mater. Sci. Technol.* **2020**, *44*, 121–132. [CrossRef]
4. Mandal, S.; Das, V.V.; Debata, M.; Panigrahi, A.; Sengupta, P.; Rajendran, A.; Pattanayak, D.K.; Basu, S. Study of pore morphology, microstructure, and cell adhesion behaviour in porous Ti-6Al-4V scaffolds. *Emerg. Mater.* **2019**, *2*, 453–462. [CrossRef]
5. Fayyad, E.M.; Abdullah, A.M.; Hassan, M.K.; Mohamed, A.M.; Jarjoura, G.; Farhat, Z. Recent advances in electroless-plated Ni-P and its composites for erosion and corrosion applications: A review. *Emerg. Mater.* **2018**, *1*, 3–24. [CrossRef]
6. Cooke, K.O.; Khan, T.I. Effect of thermal processing on the tribology of nanocrystalline Ni/TiO_2 coatings. *Emerg. Mater.* **2018**, *1*, 165–173. [CrossRef]
7. Boomadevi Janaki, G.; Xavier, J.R. Evaluation of Mechanical Properties and Corrosion Protection Performance of Surface Modified Nano-alumina Encapsulated Epoxy Coated Mild Steel. *J. Bio Tribo Corros.* **2020**, *6*, 20. [CrossRef]
8. Patel, D.; Makwana, K.; Shirdhonkar, M.B.; Kuperkar, K.C. Electrochemical response and computational approach on surface-active ionic liquid (SAIL) in metal corrosion inhibition. *Emerg. Mater.* **2020**, *3*, 161–168. [CrossRef]
9. Kannan, K.; Sivasubramanian, D.; Seetharaman, P.; Sivaperumal, S. Structural and biological properties with enhanced photocatalytic behaviour of CdO-MgO nanocomposite by microwave-assisted method Optik 2020, 204, 164221. *Optik* **2020**, *204*, 164221. [CrossRef]
10. Kannan, K.; Radhika, D.; Nikolova, M.P.; Sadasivuni, K.K.; Mahdizadeh, H.; Verma, U. Structural studies of bio-mediated NiO nanoparticles for photocatalytic and antibacterial activities. *Inorg. Chem. Commun.* **2020**, *113*, 107755. [CrossRef]
11. Kannan, K.; Radhika, D.; Vijayalakshmi, S.; Sadasivuni, K.K.; Ojiaku, A.A.; Verma, U. Facile fabrication of CuO nanoparticles via microwave-assisted method: Photocatalytic, antimicrobial and anticancer enhancing performance. *Int. J. Environ. Anal. Chem.* **2020**. [CrossRef]
12. Popoola, A.P.I.; Aigbodion, V.S.; Fayomi, O.S.I. Anti-corrosion coating of mild steel using ternary Zn-ZnO-Y2O3 electrodeposition. *Surf. Coat. Technol.* **2016**, *306*, 448–454. [CrossRef]
13. Fayomi, O.S.I.; Popoola, A.P.I.; Aigbodion, V.S. Investigation on microstructural, anti-corrosion and mechanical properties of doped Zn–Al–SnO_2 metal matrix composite coating on mild steel. *J. Alloy. Compd.* **2015**, *623*, 328–334. [CrossRef]
14. Malatji, N.; Popoola, A.P.I.; Fayomi, O.S.I.; Loto, C.A. Multifaceted incorporation of Zn-Al_2O_3/Cr_2O_3/SiO_2 nanocomposite coatings anti-corrosion tribological and thermal stability. *Int. J. Adv. Manuf. Technol.* **2016**, *82*, 1335–2134. [CrossRef]

15. Kallappa, D.; Venkatarangaiah, V.T. Synthesis of CeO_2 doped ZnO nanoparticles and their application in Zn-composite coating on mild steel. *Arab. J. Chem.* **2020**, *13*, 2309–2317. [CrossRef]
16. Wadhwani, P.M.; Ladha, D.G.; Panchal, V.K.; Shah, N.K. Enhanced corrosion inhibitive effect of p-methoxybenzylidene-4,4′-dimorpholine assembled on nickel oxide nanoparticles for mild steel in acid medium. *RSC Adv.* **2015**, *5*, 7098–7111. [CrossRef]
17. Shajudheen, V.M.; Kumar, V.S.; Maheswari, A.U.; Sivakumar, M.; Kumar, S.S.; Rani, K.A. Characterization and anticorrosion studies of spray coated nickel oxide (NiO) thin films. *Mater. Today Proceed.* **2018**, *5*, 8577–8586. [CrossRef]
18. Aruna, S.T.; Bindu, C.N.; Ezhil Selvi, V.; William Grips, V.K.; Rajam, K.S. Synthesis and properties of electrodeposited Ni/ceria nanocomposite coatings. *Surf. Coat. Technol.* **2006**, *200*, 6871–6880. [CrossRef]
19. Suresh, K.C.; Balamurugan, A. Evaluation of structural, optical, and morphological properties of nickel oxide nanoparticles for multi-functional applications. *Inorg. Nano-Metal Chem.* **2020**. [CrossRef]
20. Xue, Y.J.; Jia, X.Z.; Zhou, Y.W.; Ma, W.; Li, J.S. Tribological performance of Ni–CeO_2 composite coatings by electrodeposition. *Surf. Coat. Technol.* **2006**, *200*, 5677–5681. [CrossRef]
21. Shajudheen, V.M.; Rani, K.A.; Kumar, V.S.; Maheswari, A.U.; Sivakumar, M.; Kumar, S.S. Comparison of Anticorrosion Studies of Titanium Dioxide and Nickel Oxide Thin Films Fabricated by Spray Coating Technique. *Mater. Today Proceed.* **2018**, *5*, 8889–8898. [CrossRef]
22. Deng, S.H.; Lu, H.; Li, D.Y. Influence of UV light irradiation on the corrosion behavior of electrodeposited Ni and Cu nanocrystalline foils. *Sci. Rep.* **2020**, *10*, 3049. [CrossRef] [PubMed]
23. Karthik, K.; Revathi, V.; Tatarchuk, T. Microwave-assisted green synthesis of SnO_2 nanoparticles and their optical and photocatalytic properties. *Mol. Cryst. Liquid Cryst.* **2018**, *671*, 17–23. [CrossRef]
24. Bukkitgar, S.D.; Shetti, N.P.; Kulkarni, R.M.; Reddy, K.R.; Shukla, S.S.; Saji, V.S.; Aminabhavi, T.M. Electro-catalytic behavior of Mg-doped ZnO nano-flakes for oxidation of anti-inflammatory drug. *J. Electrochem. Soc.* **2019**, *166*, B3072–B3078. [CrossRef]
25. Xavier, J.R. Effect of surface modified WO_3 nanoparticles on the epoxy coatings for the adhesive and anticorrosion properties of mild steel. *J. Appl. Polym. Sci.* **2019**, *137*, 48323. [CrossRef]
26. Yu, Z.; Di, H.; Ma, Y.; Lv, L.; Pan, Y.; Zhang, C.; He, Y. Fabrication of graphene oxide–alumina hybrids to reinforce the anti-corrosion performance of composite epoxy coatings. *Appl. Surf. Sci.* **2015**, *351*, 986–996. [CrossRef]
27. Mirabedini, S.M.; Moradian, S.; Scantlebury, J.D.; Thompson, G.E. Characterization and corrosion performance of powder coated aluminium alloy. *Iran Polym. J.* **2003**, *12*, 261–270.
28. Hadavand, B.S.; Ataeefard, M.; Bafghi, H.F. Preparation of modified nano ZnO/polyester/TGIC powder coating nanocomposite and evaluation of its antibacterial activity. *Compos. Part B Eng.* **2015**, *82*, 190–195. [CrossRef]
29. Ashassi-Sorkhabi, H.; Seifzadeh, D.; Raghibi-Boroujeni, M. Analysis of electrochemical noise data in both time and frequency domains to evaluate the effect of ZnO nanopowder addition on the corrosion protection performance of epoxy coatings. *Arab. J. Chem.* **2016**, *9*, S1320–S1327. [CrossRef]
30. Xavier, J.R. Application of EIS and SECM studies for investigation of anticorrosion properties of epoxy coatings containing zinc oxide nanoparticles on mild steel in 3.5% NaCl solution. *J. Mater. Eng. Perform.* **2017**, *26*, 3245–3253.
31. Madhankumar, A.; Ramakrishna, S.; Sudhagar, P.; Kim, H.; Kang, Y.S.; Obot, I.B.; Gasem, Z.M.A. An electrochemical, in vitro bioactivity and quantum chemical approach to nanostructured copolymer coatings for orthopedic applications. *J. Mater. Sci.* **2014**, *49*, 4067–4080. [CrossRef]
32. Jeyasubramanian, K.; Benitha, V.S.; Parkavi, V. Nano iron oxide dispersed alkyd coating as an efficient anticorrosive coating for industrial structures. *Prog. Org. Coat.* **2019**, *132*, 76–85. [CrossRef]
33. Krishnan, A.; Joseph, B.; Bhaskar, K.M.; Suma, M.S.; Shibli, S.M.A. Unfolding the anticorrosive characteristics of TiO_2–WO_3 mixed oxide reinforced polyaniline composite coated mild steel in alkaline environment. *Polym. Compos.* **2018**, *40*, 2400–2409. [CrossRef]
34. Al-Gamal, A.G.; Farag, A.A.; Elnaggar, E.M.; Kabel, K.I. Comparative impact of doping nano-conducting polymer with carbon and carbon oxide composites in alkyd binder as anti-corrosive coatings. *Compos. Interfaces* **2018**, *25*, 959–980. [CrossRef]

35. Pourhashem, S.; Vaezi, M.R.; Rashidi, A.; Bagherzadeh, M.R. Exploring corrosion protection properties of solvent based epoxy-graphene oxide nanocomposite coatings on mild steel. *Corros. Sci.* **2016**, *115*, 78–92. [CrossRef]
36. Deshpande, P.P.; Jadhav, N.G.; Gelling, V.J.; Sazou, D. Conducting polymers for corrosion protection: A review. *J. Coat. Technol. Res.* **2014**, *11*, 473–494. [CrossRef]
37. Ghasemi-Kahrizsangi, A.; Shariatpanahi, H.; Neshati, J.; Akbarinezhad, E. Corrosion behavior of modified nano carbon black/epoxy coating in accelerated conditions. *Appl. Surf. Sci.* **2015**, *331*, 115–126. [CrossRef]
38. Wu, L.K.; Zhang, J.T.; Hu, J.M.; Zhang, J.Q. Improved corrosion performance of electrophoretic coatings by silane addition. *Corros. Sci.* **2012**, *56*, 58–66. [CrossRef]
39. Bayat, S.; Jazani, O.M.; Molla-Abbasi, P.; Jouyandeh, M.; Saeb, M.R. Thin films of epoxy adhesives containing recycled polymers and graphene oxide nanoflakes for metal/polymer composite interface. *Prog. Org. Coat.* **2019**, *136*, 105201. [CrossRef]
40. Xavier, J.R. Investigation on the anticorrosion, adhesion and mechanical performance of epoxy nanocomposite coatings containing epoxy-silane treated nano MoO_3 on mild steel. *J. Adhes. Sci. Technol.* **2020**, *34*, 115–134. [CrossRef]
41. Shen, G.X.; Chen, Y.C.; Lin, C.J. Corrosion protection of 316L stainless steel by a TiO_2 nanoparticles coating prepared by sol–gel method. *Thin Solid Films* **2005**, *489*, 130–136. [CrossRef]
42. Shan, C.X.; Hou, X.; Choy, K.L.; Choquet, P. Improvement in corrosion resistance of CrN coated stainless steel by conformal TiO_2 deposition. *Surf. Coat. Technol.* **2008**, *202*, 2147–2151. [CrossRef]
43. Díaz, B.; Światowska, J.; Maurice, V.; Pisarek, M.; Seyeux, A.; Zanna, S.; Tervakangas, S.; Kolehmainen, J.; Marcus, P. Chromium and tantalum oxide nanocoatings prepared by filtered cathodic arc deposition for corrosion protection of carbon steel. *Surf. Coat. Technol.* **2012**, *206*, 3903–3910. [CrossRef]
44. Mirhashemihaghighi, S.; Światowska, J.; Maurice, V.; Seyeux, A.; Klein, L.H.; Salmi, E.; Ritala, M.; Marcus, P. The role of surface preparation in corrosion protection of copper with nanometer-thick ALD alumina coatings. *Appl. Surf. Sci.* **2016**, *387*, 1054–1061. [CrossRef]
45. Nouri, E.; Shahmiri, M.; Rezaie, H.R.; Talayian, F. Investigation of structural evolution and electrochemical behaviour of zirconia thin films on the 316L stainless steel substrate formed via sol–gel process. *Surf. Coat. Technol.* **2011**, *205*, 5109–5115. [CrossRef]
46. Fayyad, E.M.; Sadasivuni, K.K.; Ponnamma, D.; Al-Maadeed, M.A.A. Oleic acid-grafted chitosan/graphene oxide composite coating for corrosion protection of carbon steel. *Carbohydr. Polym.* **2016**, *151*, 871–878. [CrossRef]
47. Mahato, N.; Cho, M.H. Graphene integrated polyaniline nanostructured composite coating for protecting steels from corrosion: Synthesis, characterization, and protection mechanism of the coating material in acidic environment. *Constr. Build. Mater.* **2016**, *115*, 618–633. [CrossRef]
48. Feng, Q.; Li, T.; Teng, H.; Zhang, X.; Zhang, Y.; Liu, C.; Jin, J. Investigation on the corrosion and oxidation resistance of Ni-Al2O_3 nano-composite coatings prepared by sediment co-deposition. *Surf. Coat. Technol.* **2008**, *202*, 4137–4144. [CrossRef]
49. Benea, L.; Luigi, P.; Borello, A.; Martelli, S. Wear corrosion properties of nano-structured SiC-nickel composite coatings obtained by electroplating. *Wear* **2002**, *249*, 995–1003. [CrossRef]
50. Ranganatha, S.; Venkatesha, T.V.; Vathsala, K. Development of electroless Ni-Zn-P/nano-TiO_2 composite coatings and their properties. *Appl. Surf. Sci.* **2010**, *256*, 7377–7383. [CrossRef]
51. Cai, C.; Zhu, X.B.; Zheng, G.Q.; Yuan, Y.N.; Huang, X.Q.; Cao, F.H.; Yang, J.F.; Zhang, B. Electrodeposition and characterization of nano-structured Ni-SiC composite films. *Surf. Coat. Technol.* **2011**, *205*, 3448–3454. [CrossRef]
52. Bigdeli, F.; Allahkaram, S.R. An investigation on corrosion resistance of as-applied and heat treated Ni-P/nanoSiC coatings. *Mater. Des.* **2009**, *30*, 4450–4453. [CrossRef]
53. Rabizadeh, T.; Allahkaram, S.R. Corrosion resistance enhancement of Ni-P electroless coatings by incorporation of nano-SiO_2 particles. *Mater. Des.* **2011**, *32*, 133–138. [CrossRef]
54. Xavier, J.R. Investigation into the effect of Cr_2O_3 nanoparticles on the protective properties of epoxy coatings on carbon steel in NaCl solution by scanning electrochemical microscopy. *Prot. Met. Phys. Chem.* **2019**, *55*, 80–88. [CrossRef]

55. Nine, M.J.; Cole, M.A.; Johnson, L.; Tran, D.N.; Losic, D. Robust superhydrophobic graphene-based composite coatings with self-cleaning and corrosion barrier properties. *ACS Appl. Mater. Interfaces* **2015**, *7*, 28482–28493. [CrossRef] [PubMed]
56. Kannan, K.; Sliem, M.H.; Abdullah, A.M.; Sadasivuni, K.K.; Kumar, B. Fabrication of ZnO-Fe-MXene Based Nanocomposites for Efficient CO_2 Reduction. *Catalysts* **2020**, *10*, 549. [CrossRef]
57. Kannan, K.; Sadasivuni, K.K.; Abdullah, A.M.; Kumar, B. Current Trends in MXene-Based Nanomaterials for Energy Storage and Conversion System: A Mini Review. *Catalysts* **2020**, *10*, 495. [CrossRef]
58. Jamwal, A.; Prakash, P.; Kumar, D.; Singh, N.; Sadasivuni, K.K.; Harshit, K.; Gupta, S.; Gupta, P. Microstructure, wear and corrosion characteristics of Cu matrix reinforced SiC–graphite hybrid composites. *J. Compos. Mater.* **2019**, *53*, 2545–2553. [CrossRef]
59. Bandil, K.; Vashisth, H.; Kumar, S.; Verma, L.; Jamwal, A.; Kumar, D.; Singh, N.; Sadasivuni, K.K.; Gupta, P. Microstructural, mechanical and corrosion behaviour of Al–Si alloy reinforced with SiC metal matrix composite. *J. Compos. Mater.* **2019**, *53*, 4215–4223. [CrossRef]
60. Ejenstam, L.; Tuominen, M.; Haapanen, J.; Mäkelä, J.M.; Pan, J.; Swerin, A.; Claesson, P.M. Long-term corrosion protection by a thin nano-composite coating. *Appl. Surf. Sci.* **2015**, *357*, 2333–2342. [CrossRef]
61. Kinlen, P.J.; Silverman, D.C.; Jeffreys, C.R. Corrosion protection using polyamine coating formulations. *Synth. Met.* **1997**, *85*, 1327–1332. [CrossRef]
62. Chen, L.; Song, R.G.; Li, X.W.; Guo, Y.Q.; Wang, C.; Jiang, Y. The improvement of corrosion resistance of fluoropolymer coatings by SiO2/poly(styrene-co-butyl acrylate) nanocomposite particles. *Appl. Surf. Sci.* **2015**, *353*, 254–262. [CrossRef]
63. Dhoke, S.K.; Mangal Sinha, T.J.; Khanna, A.S. Effect of nano-Fe_2O_3 particles on the corrosion behavior of alkyd based waterborne coatings. *J. Coat. Technol. Res.* **2009**, *6*, 353–368. [CrossRef]
64. Dhoke, S.K.; Khanna, A.S.; Sinha, T.J.M. Effect of nano-ZnO particles on the corrosion behavior of alkyd-based waterborne coatings. *Progress Org. Coat.* **2009**, *64*, 371–382. [CrossRef]
65. Vaezi, M.R.; Sadrnezhaad, S.K.; Nikzad, L. Electrodeposition of Ni-SiC nano-composite coatings and evaluation of wear and corrosion resistance and electroplating characteristics. *Colloids Surf. A Physicochem. Eng. Asp.* **2008**, *315*, 176–182. [CrossRef]
66. Allahkaram, S.R.; Nazari, M.H.; Mamaghani, S.; Zarebidaki, A. Characterization and corrosion behavior of electroless Ni-P/nano-SiC coating inside the CO_2 containing media in the presence of acetic acid. *Mater. Des.* **2011**, *32*, 750–755. [CrossRef]
67. Feng, L.; Yuan, P. Corrosion protection mechanism of aluminum triphosphate modified by organic acids as a rust converter. *Prog. Org. Coat.* **2020**, *140*, 105508. [CrossRef]
68. Gobara, M.; Baraka, A.; Akid, R.; Zorainy, M. Corrosion protection mechanism of Ce^{4+}/organic inhibitor for AA2024 in 3.5% NaCl. *RSC Adv.* **2020**, *10*, 2227–2240. [CrossRef]